Damage Sensitive-Stories of RC and Steel Frames under Critical Mainshock-Aftershock Ground Motions

Elham Rajabi[1]*, Gholamreza Ghodrati Amiri[2]

1. Department of Civil Engineering, Tafresh University, Tafresh 39518–79611, Iran
2. Natural Disasters Prevention Research Center, School of Civil Engineering, Iran University of Science & Technology, PO Box 16765-163, Narmak, Tehran 16846, Iran
Corresponding author: rajabi@tafreshu.ac.ir

ARTICLE INFO

ABSTRACT

Cumulated damages caused by the past earthquakes lead to structural damage. Ensuring the safety of individuals – especially in highly populated buildings – and the continuity of immediate occupancy in consecutive earthquakes with short periods is an important matter to consider in seismic design codes. The use of strategies, such as identifying damage sensitive stories, can help ensure the safety of such buildings. This paper identifies damage sensitive stories for reinforced concrete (RC) and steel frames based on damage distribution caused by critical mainshock-aftershocks. In this regard, short, medium and relatively tall steel and RC frames with 3 and 5, 7, 10, 12 and 15 stories are analyzed under single and successive scenarios in the OpenSees software. Damage distribution of frames show that the upper stories in frames with low and medium height and middle stories toward higher stories in relatively tall frames are damage sensitive stories. Also, when tested against successive shocks, the initially-damaged steel frames experienced more destruction than RC frames. In severe conditions, the increased damages of steel frames were about 57%, 94%, 42%, 33% and 84% more than those of the RC frames. Moreover, steel frames with 15 stories were better able to sustain additional damages than RC frames (by about 1.84 times).

---

1. Introduction

While the second shocks in seismic scenarios with main shock-aftershock usually have a smaller magnitude than the initial shocks, the intensity of the aftershock is not necessarily less. In fact, the main shocks may even have smaller peak ground accelerations (PGA), dissimilar content of energy and shorter durations than the aftershocks. Intact buildings have even shown to collapse after successive shocks due to a significant reduction of structural capacity. For example, the Sarpol-e Zahab earthquake (a strong earthquake with Mw 7.3 - 2017) –the second strongest earthquake after the M7.4 of the 1909 AD Sialkhor earthquake – had more than 900 aftershocks.

While earthquakes with foreshocks generally lead to lesser human casualties as people are able to leave their homes before the main shock, the single earthquakes are considered in the design process of buildings which have been founded on seismic active zones and can lead to a non-conservative prediction of seismic risk. Nonetheless, most buildings are still designed or retrofitted to suit the single earthquake based on seismic design codes, when in fact repeated earthquakes strongly affect the capacity of structures.

The literature on structural and earthquake engineering [1-5] present the necessity of the seismic sequence phenomena and propose approaches to consider the effects of successive earthquakes. In this regard, Zhang et al. [6] presented a new methodology to develop state-dependent fragility curves for wood-frame houses founded on British Columbia, Canada under real mainshock-aftershock records. The fragility curves, which have been developed for considering the damage accumulation, provide the exceeding probability of the damage state corresponding to the seismic event intensity measure and the structural damage state prior to the seismic scenarios. The results of their study indicate that state-dependent fragility curves, based on the residual and maximum inter-story drift ratio and peak ground velocity, are the proper selection for determining the cumulative damage effects [6].

In the same year, Wen et al. [7] quantified the cumulative damage of structures considering the effects of aftershocks with pulse specifications. They claimed that strong near-fault aftershocks can increase the cumulative damage by about 40%. Also, in order to predict the damage caused by pulse-like main shock - aftershock sequences, several equations were proposed [7].

Zhai et al. [8] studied post-mainshock damage states by evaluating additional accumulative damages of containment structures caused by aftershocks with various durations. Their study found accumulative damages caused by aftershocks with longer durations to be more severe. It can thus be said that accurate evaluation of the containment structures, safety depends on the aftershock features and duration. Aftershocks should, therefore, be taken into account when selecting ground motion records for seismic safety assessment of a Nuclear Power Plant [8].

Since soft soil has considerable amplification effects on ground motions, Wen et al. [9] proposed a spectrum for damage caused by main shock-aftershock at soft soil sites to evaluate the accumulated damage experienced by the structures under these sequences. They mentioned that the strong aftershocks at soft soil sites can increase the spectrum of damage by more than forty percent. Also, strong aftershocks at firm soil sites cause smaller additional damage than those at soft soil sites [9]. Zhang et al. [10] investigated the strength

reduction factor of a single-degree-of-freedom (SDOF) system under successive earthquakes by considering displacement ductility and cumulative damages. The results indicated that aftershock ground motions significantly affect strength reduction factors, and the damage-based strength reduction factor is about 0.6–0.9 times the ductility-based strength reduction factor [10].

In addition to the above researches [7-9], many other recent studies [11-12] have also investigated the damage caused by consecutive earthquakes. Ghaderi and Gholizadeh [11] conducted a numerical assessment of steel moment frames (SMFs) for low-cycle fatigue (LCF) damage under mainshock-aftershock and found that the repeated earthquakes strongly affect the inelastic response and vulnerability of structures. The Palmgren-Miner's rule was applied to the relative drift of the stories and the LCF damage index for SMFs was calculated under real strong multiple earthquakes. In order to increase the safety of optimally designed SMFs against LCF damage, Ghaderi and Gholizadeh proposed a simple procedure and examined the effectiveness of the strategy in controlling the LCF damage of SMFs caused by successive earthquakes [11].

In most studies, artificial earthquakes which have been generated by "random" and "back to back" approaches are used to consider the seismic sequence phenomena. It should be noted, the use of artificial approaches can cause a non-conservative prediction of structural performance [13].

Damage caused by critical successive earthquakes is one of the most important parameters in the examination of accumulated damages and realistic behavior of structures. Also, identification of damage sensitive stories is possible based on damage distribution along the height of the structure.

Consequently, providing damage control in these stories can strongly improve the safety of the people. For this purpose, this paper evaluates the damage sensitive-stories of RC and steel frames under real critical mainshock-aftershock ground motions. Two sets of steel and RC moment resisting frames with 3, 5, 7, 10, 12 and 15 stories were designed in the OpenSees software, and the stiffness and strength deterioration properties were analyzed under a significant number of real critical seismic scenarios in "single" and "consecutive" cases. These scenarios are scaled based on the design spectrum for each fundamental period to achieve more realistic results. The single and consecutive scenarios damage of all RC and steel frames for each floor is calculated using the Park and Ang's damage index [14], and the results are compared for several cases. Comparison of the results show that increased damages of RC frames are about 40% less than those of steel frames in the most severe conditions. Moreover, the steel frames with 15 stories sustained 1.84 times more damages than RC frames.

2. Research methodology

2.1. Strong ground motions

This research investigates RC and steel frames under main shock as well as the distribution of damage caused by aftershocks. 84 critical recorded earthquakes with one aftershock were selected and used based on the effective peak acceleration (EPA) from the PEER [16] and USGS [17] centers. EPA is proposed as one of the most suitable parameters for selecting the critical earthquake [15]. It is the mean value of the acceleration response spectrum (for 5% damping) for periods between 0.1 and 0.5 (s) divided by the standard amplification coefficient, 2.50. In addition, the EPA

parameter indicates the amplitude and the frequency content of the ground motion. The EPA parameter was calculated for all of the successive earthquakes, and the seismic scenarios were divided to two databases with time gaps of less than 10 minutes and 10 days (the criterion for the selection of these numbers - 10 minutes and 10 days - is adequate opportunity for initial excavation of buildings and primary repairs of structures after main-shocks).

The EPA parameter was determined for all of the seismic scenarios with sequence phenomena and time gaps of less than 10 minutes and 10 days.

The earthquakes with/without the following shocks have Max EPA[1] and App EPA[2] – second or third rank relative to the maximum value – in each database [18]. In fact, the purpose of this selection (Max EPA and App EPA) was to determine the structural response and behavior of damage sensitive-stories under successive earthquakes with severe intensities. More details and list of earthquakes are available in the works of Ghodrati Amiri and Rajabi [18].

It should be noted that the seismic scenarios are scaled to have identical spectral acceleration with the design spectrum for the fundamental period of each frame. For this purpose, all ground motion records are scaled using linear scaling [19] by multiplying time histories by the suitable factor [20]. The mentioned technique is convenient for implementation, as it helps sustain the original phasing and frequency content of the earthquakes [21]. The

acceleration response spectra and the corresponding mean spectrum of critical successive scenarios for analyzing the RC and steel frames are shown in Fig.1. Also, the specification of earthquakes in the aforementioned database with a time gap of less than 10 minutes and 10 days is presented in the works of Ghodrati Amiri and Rajabi [18].

As mentioned above, the first and second databases differ in terms of the time intervals between the critical consecutive shocks. Successive shocks in the first database followed each other by real time gap (less than 10 minutes), while the critical successive shocks in the second database were recorded under 10 days of each other. It can thus be concluded that the real time gap (more than one day) increases the volume of the nonlinear dynamic analysis, making the damage index calculation process very time consuming. For this reason, an artificial time interval equal to 120 (s) is considered for successive earthquakes in the second database. This time interval is sufficient to stop the motion of the structure due of the damping, and it is selected after examining the time gap effects on the damage index of RC frames.

Structural damages caused by the recorded successive earthquakes were, therefore, calculated by considering different time gaps between the main-shock and aftershock, which started from 20 (s) to real time gap with time intervals of 5 (s). For example, Fig. 2(a) shows the variation of the damage index with a time gap between successive shocks.

---

[1] Maximum EPA
[2] Approximately maximum EPA

(a) Less than 10 minutes.   (b) Less than 10 days.
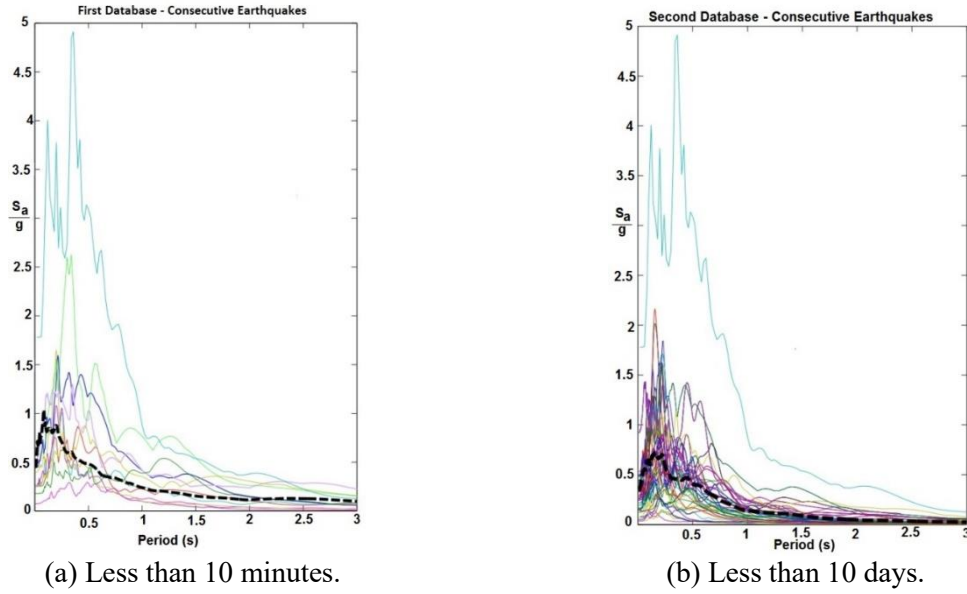
Fig. 1. Acceleration response spectra and the corresponding mean spectrum with time gap.
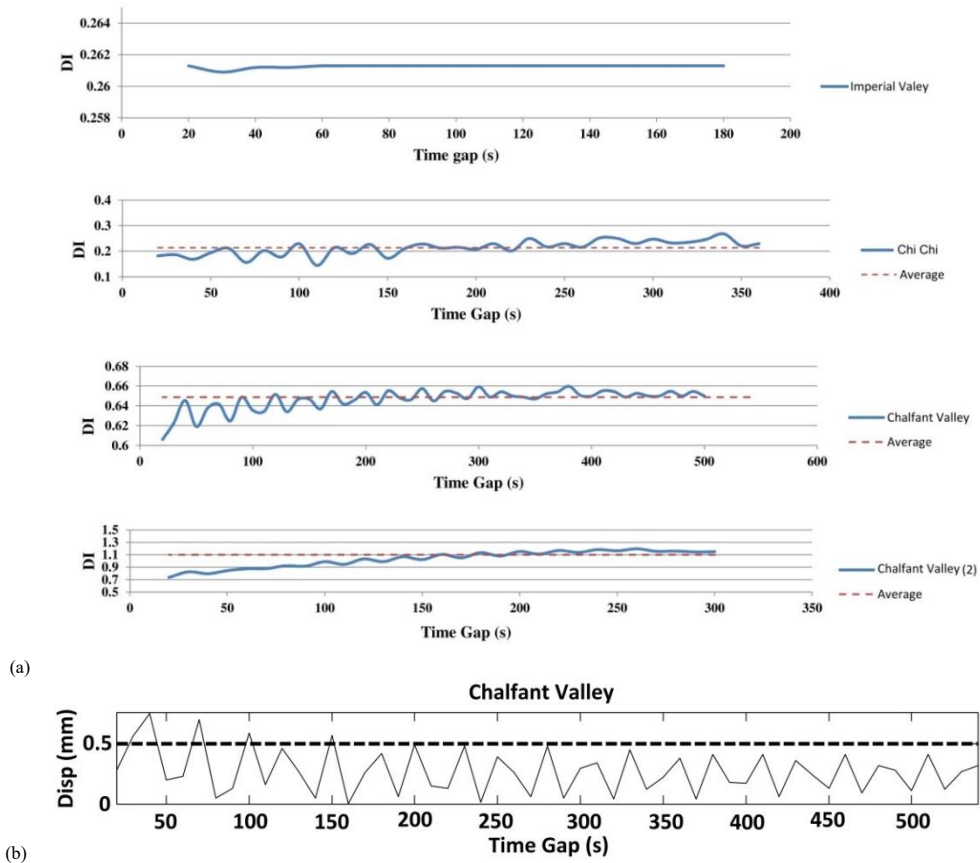
Fig. 2. (a) Damage index of 5 story RC frame under several consecutive earthquakes with different time gap between successive shocks and (b) Displacement under the Chalfant Valley earthquake (1986).

The damage indices were caused by the Imperial Valley, Chi Chi and the Chalfant Valley 1 and 2 earthquakes in five-story RC frames. As shown in this figure, the rate of the damage index variation is almost fixed after 120 (s). In fact, the studied frames stop at about 120 (s) after the first shock because the displacement of these frames significantly reduced to less than 1.0 mm. Fig. 2(b) illustrates the RC frame with 5 stories displacement versus the time gap for the Chalfant Valley earthquake. Partial displacements are considered in numerical calculations, and some fluctuations are observed in some parts of the curve. Nevertheless, the structure is assumed to be practically motionless after 120 seconds, and the rate of the damage index variation can be considered almost fixed after this time. In other words, the time gap does not have much effect on the damage index at the end of the building motion. It should also be mentioned that although the time gap of 10 minutes and 120 seconds is both enough to stop the vibration of the first shock-damaged structures before the occurrence of the second shock, successive earthquakes with time gaps of 10 minutes are considered in the separate group (1st Database) to study the performance of RC and steel frames under more realistic conditions.

2.2. Reinforced concrete and steel frames

Two dimension reinforced concrete and steel moment frames – of short with 3 and 5, medium with 7 and 10 and relatively tall frames with 12 and 15 stories and fixed base – which have been used in Ghodrati and Rajabi [18] is analyzed under all scaled earthquakes in single and consecutive cases. The schematic elevation of the studied frames is shown in Fig.3. It should be noted

that, all frames are designed based on the Standard 2800[3] and analyzed in the *open source* platform after verifying the analytical and experimental results of Lignos et al. [22] for steel frames and Nagaee et al. [23] for RC frames.

The properties of the used frames are introduced in [18] and the Appendix. Simulation of the flexural behavior of the frames in the nonlinear case is modeled using concentrated plastic hinges in the beams and fiber section for the columns. In this regard, the modeling of the beams and columns are performed using the "beam with hinge element" and the "nonlinear beam column element", in the Opensees software, respectively. According to Ghodrati and Rajabi [18], the backbone curve with three lines, proposed by Haselton et al. [24] and Moehle et al. [25], is used for modeling the beams in reinforced concrete and steel frames, respectively. Important features of RC frames [26] are shown in Fig. 4. The Clough material proposed by Altoontash [24] is used for tri-linear models in the Opensees software. More details are discussed in Ghodrati and Rajabi [18].

3. Results of damage index

Damage prediction in buildings can be used as a useful tool for managing and decreasing the seismic risk of earthquakes.

---

[3] Iranian Code of Practice for Seismic Resistant Design of Buildings
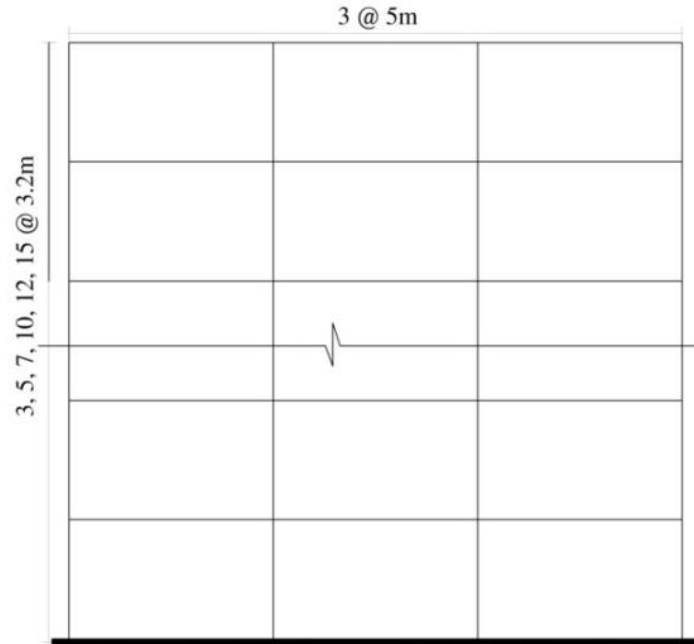
Fig. 3. The schematic elevation of the studied frames [18].

(a) Basic strength.
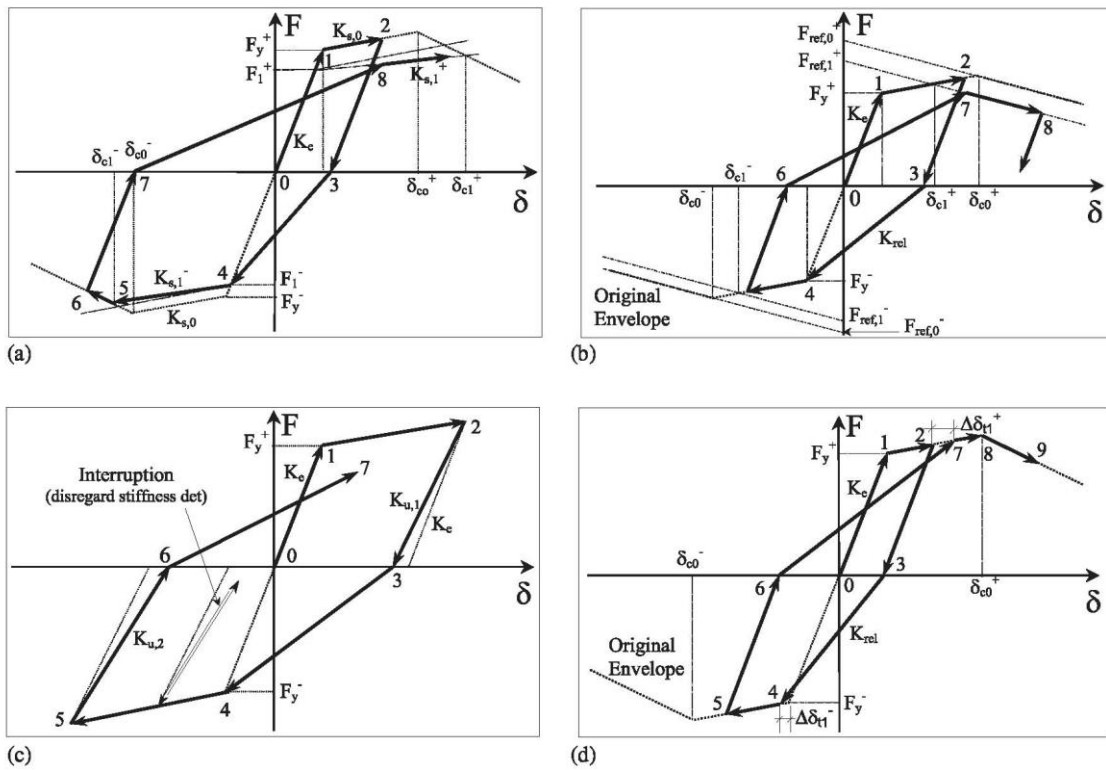
(c) Un-loading stiffness.

(b) Post-capping strength.

(d) Accelerated reloading stiffness.

Fig. 4. Deterioration modes in concrete models [26].

This paper examines sensitive stories to damage that have been identified based on the damage distribution caused by critical mainshock-aftershock ground motions. Engineering literature presents many forms of damage index definitions, most of which are presented based on simple concepts, such as ductility ratio and inter-story drift. The damage index proposed by Park and Ang [14] is the most simple and commonly used index, and most recent indices are developed with regards to the Park and Ang index [27-28], which is defined based on the linear combination of the dissipated energy and maximum displacement. Moreover, some researchers [29-32] used the Park-Ang damage index to report the results. The Park-Ang damage index was used in this research to investigate the damage sensitive stories based on the distribution of damage caused by aftershocks in the main shock-damage RC and steel frames [14]:

$$DI = \frac{\delta_m}{\delta_u} + \frac{\beta}{P_y\,\delta_u} \int dE_h \qquad (1)$$

In this equation, δ_m is the maximum element deformation, δ_u is the ultimate deformation (calculated based on Pushover analysis), β is a constant parameter as controller of strength deterioration and usually assumed between 0.05 to 0.20, $\int dE$ is the absorbed energy of elements in the earthquake, and P_y is the strength related to the yield state of the element (calculated based on the Pushover analysis). In this paper, β is taken as 0.15 and 0.025 according to [33], [34] and [35] for RC and steel frames, respectively.

In order to calculate this index under seismic excitation with/without sequence, the control node was selected at the center of mass at each story of RC and steel frames. Distribution of the damage index ratio is seen at the height of the RC and steel frames in Figs. 5 and 6. In these figures, horizontal axes present the ratio of the damage index caused by critical successive earthquakes to critical single earthquakes (DI Ratio). This ratio is shown for three cases: (1) first database, (2) second database, and (3) the average of (1) and (2). These figures show that the damages caused by successive earthquakes in all of the stories are more than those caused by single earthquakes (DI Ratio≥1). Because the frames developed more slender hysteresis loops against single earthquakes and the absorbed energy in earthquakes is the effective factor in calculating the proposed damage index by Park and Ang, the structural damage caused by the mainshock-aftershock sequence was larger than that of the single scenarios. The rate of this increase was larger for repeated shocks with smaller time gaps in the second database.

For a more realistic investigation of the critical ground motion effects ‑ in terms of intensity (Max EPA) and time interval between successive shocks (time gap equal 120 seconds) on the increased damage in stories ‑ distribution of damage caused by worst case scenarios ‑ critical successive shocks with Max EPA and short period ‑ are compared in Fig. 7 for RC and steel frames. Although the variation trend of damages is more gradual in steel frames than in RC frames, shorter steel and especially RC frames (3, 5 and 7 stories) and relatively tall frames (10, 12 and 15 stories) sustain more damages in the upper and middle floors, respectively, due to the occurrence of critical aftershocks with maximum EPA.

RC   Steel
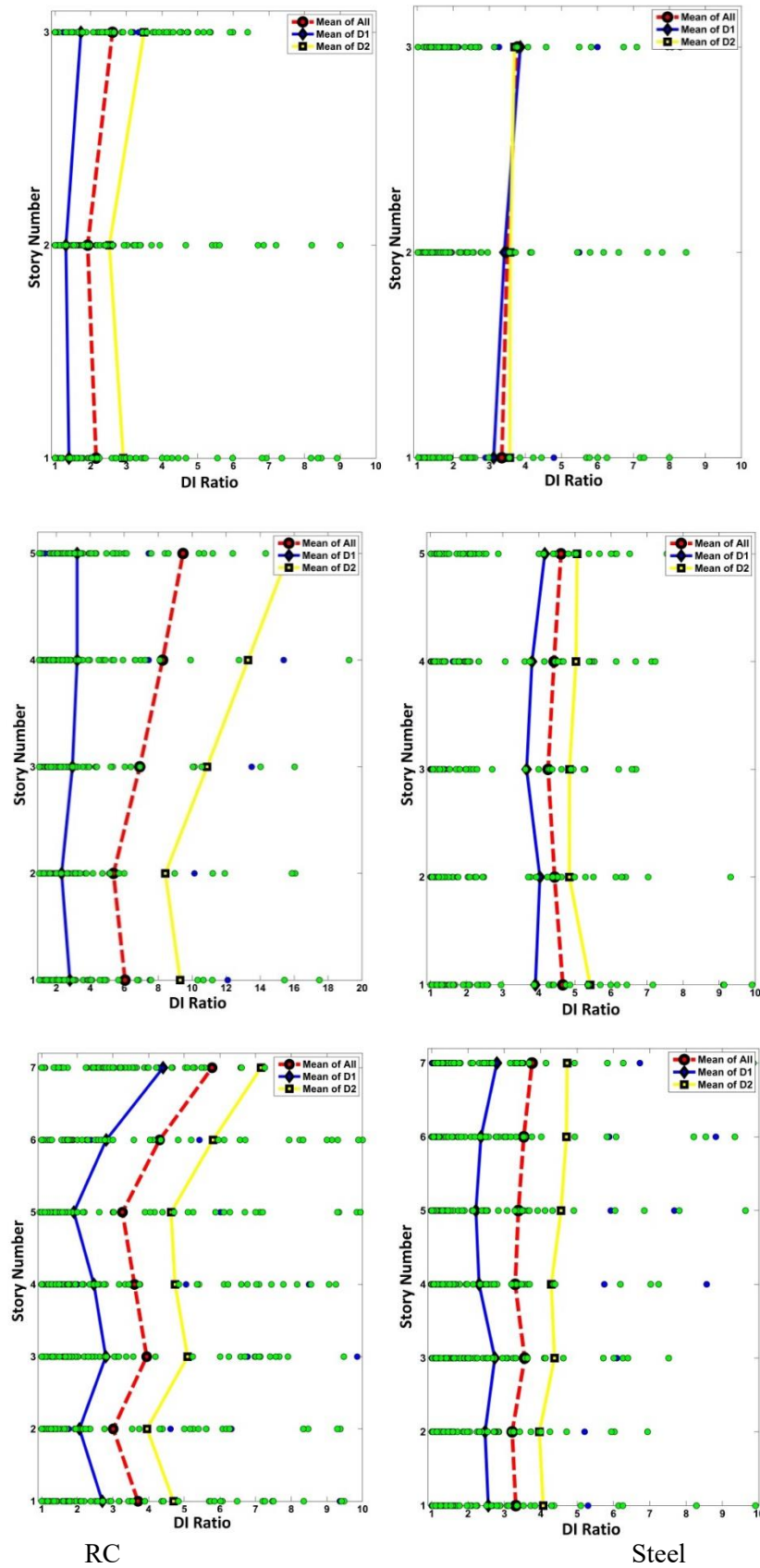
Fig. 5. Distribution of DI ratio in the height of frames with 3, 5 and 7 story.

RC   Steel
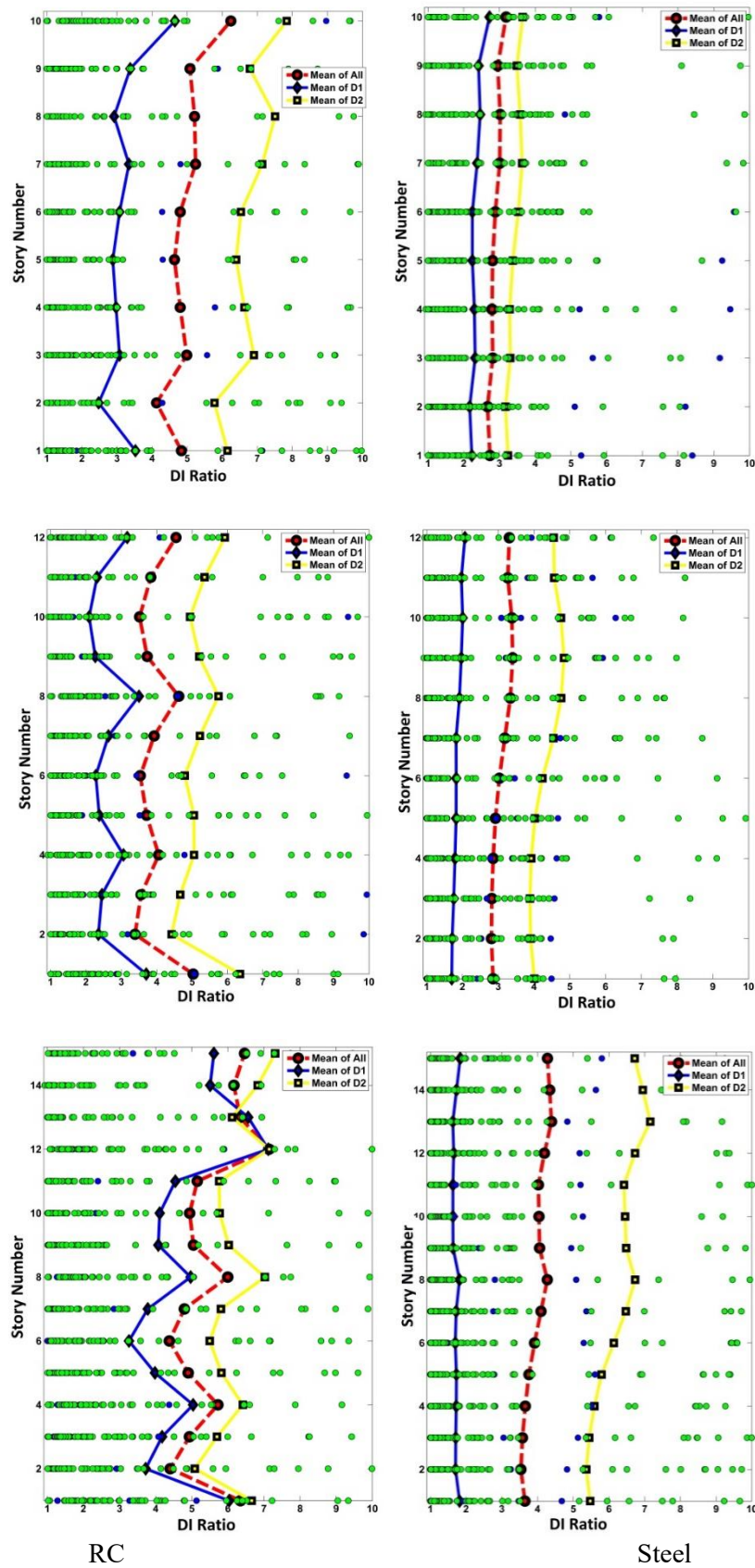
Fig. 6. Distribution of DI ratio in the height of 10, 12 and 15 story frames.
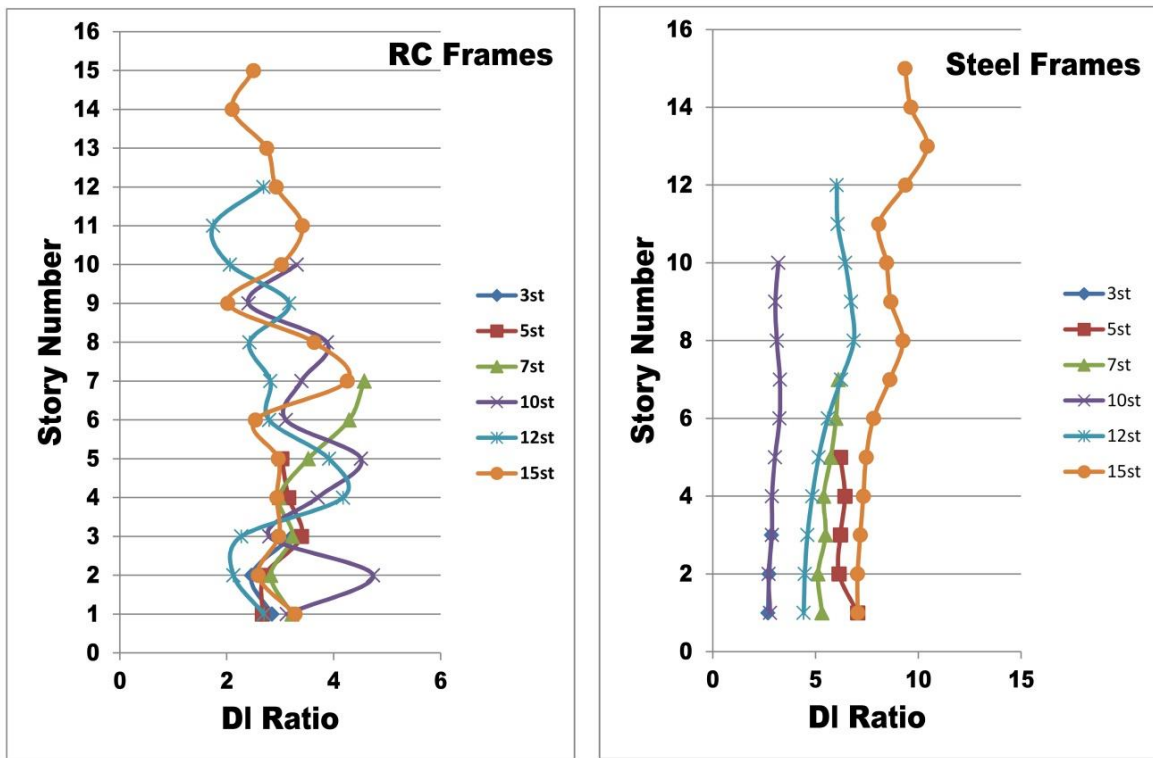
Fig. 7. Mean of the damage index ratio caused by critical successive earthquake to critical single earthquake with maximum EPA and time gap 120 s.

Maximum deformations are likely recorded in the upper floors in short frames. Also, damages in middle stories can be affected more by changing the section classification and, consequently, the story stiffness and area under the hysteresis loops. The following section identifies the damage sensitive stories that experienced successive earthquakes with time gaps of less than 10 minutes and 10 days. Fig. 8 shows the average of the damage index ratio caused by all critical successive earthquakes to the critical single earthquake in each story using bars. For better comparison, bars related to low and medium frames are displayed in one figure. As shown in this figure, the upper stories in the RC and steel frames with low and medium height and middle stories toward higher stories in relatively tall RC and steel frames are also considered damage sensitive stories.

Fig. 9 compares the performance of damaged stories in steel frames with that of RC frames based on the average of damage distribution under all critical scenarios and story number. As seen in this figure, RC frames perform better against critical aftershocks. Since the hysteresis energy absorbed during the earthquake (E) is one of the most effective parameters on the Park Ang damage index (based on Eq. (1)), the steel frames have formed wider hysteresis loops than RC frames under single and successive earthquakes, and RC frames experience less damage than steel frames under the seismic sequence phenomena. In the most severe conditions, increased damages of steel frames are about 57%, 94%, 42%, 33% and 84% more than those of RC frames under critical consecutive earthquakes.

(a)

(b)
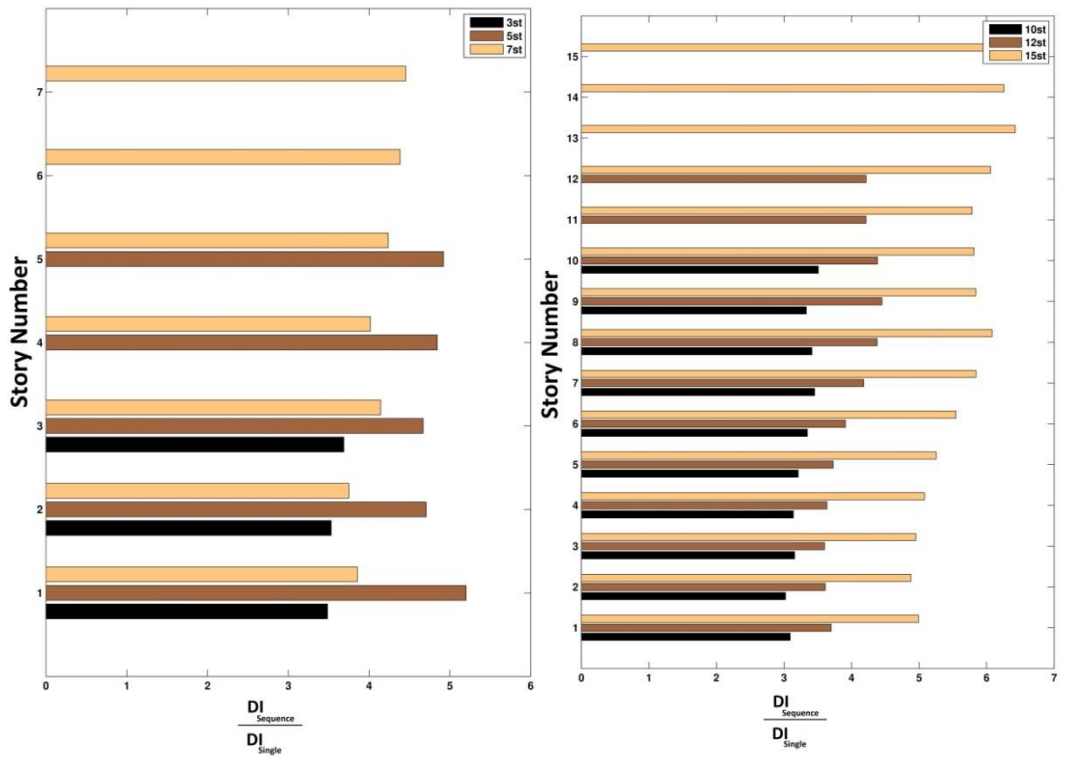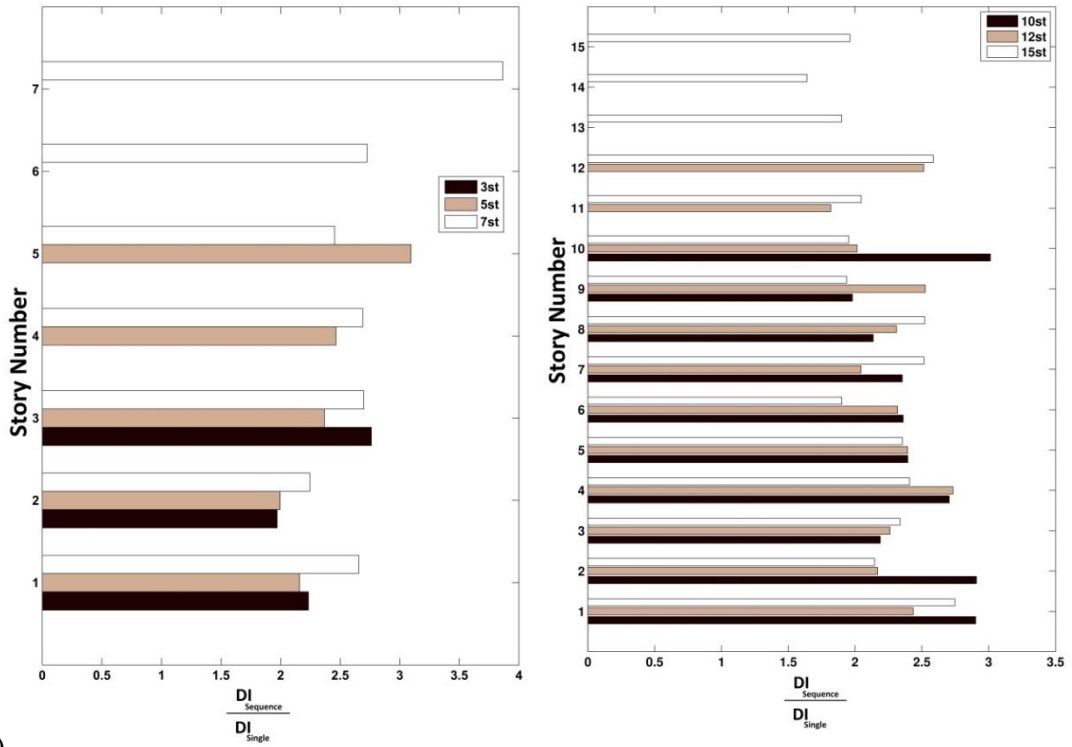
Fig. 8. Mean of damage index ratio caused by all critical successive earthquakes to critical single earthquakes in (a) RC and (b) Steel frames.
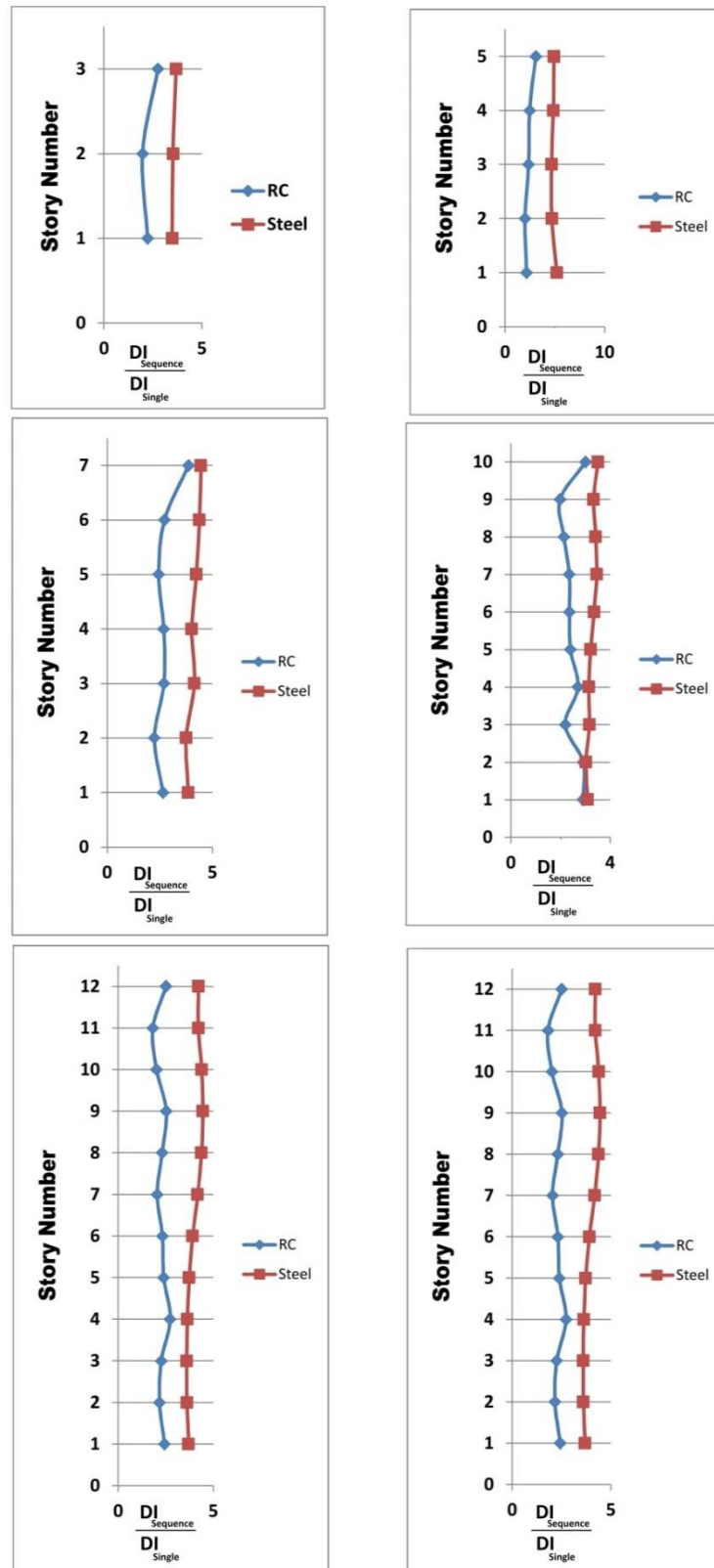
Fig. 9. The average of DI for steel and RC frame against all of critical earthquakes.

Moreover, additional damage in steel frames with 15 stories is about 1.84 times more than RC frames.

Finally, the average of the increased damage index ratio ($R = DI_{Sequence}/DI_{Single}$) for steel to RC frames (R_{Steel}/R_{RC}) is compared in Fig. 10, based on the number of stories. As seen in this figure, cumulative damages are caused by repeated shocks that were previously divided into two databases. The last bar in each figure presents the mean of this ratio for all stories. Fig. 10 illustrates that this ratio is always larger than one, which shows that RC frames perform better than steel frames under consecutive earthquakes. Regardless of the number of stories, results reveal that when confronted with critical consecutive shocks, RC frames are about 48% less vulnerable than steel frames.

4. Conclusions

This paper investigates the damage sensitive-stories for regular reinforced concrete and steel frames under successive ground motions because seismic sequence phenomenon has significantly effects on the response and behavior of structures. In addition to, determination of these stories location and utilization of retrofitting methods can decrease the additional damages in multiple earthquakes. In this regard, short - with 3 and 5-, medium - with 7 and 10-, relatively tall steel and RC frames with 12 and 15 stories have been designed and analyzed by real critical earthquakes in single and successive cases which have been scaled based on design spectrum. Damage caused by these earthquakes in all floors of steel and RC frames is determined based on Park-Ang damage index [14]. Based on the obtained result in this paper, the conclusions are:

- Despite what is often assumed in the seismic design codes, earthquakes do not occur as a single event. In seismic active zones, earthquakes consist of numerous consecutive shocks which can cause the additional cumulative damage to structures. For this reason, disregarding the successive earthquakes in the structural design will be irreparable.

- As decreasing the time interval between shocks, cumulative structural damage will be increased.

- The comparison between the performance of frames under critical ground motions shows that steel frames have poor performance in general. Steel frames have been formed wider hysteresis loops rather than RC frames under single and successive earthquake. Therefore hysteresis energy absorbed during the earthquake and damage index increased.

- Shorter and medium RC and steel frames (3, 5, 7 and 10 stories) and relatively tall frames (12 and 15 stories) sustain more damages in upper floors and middle floors respectively under critical successive records with Max EPA and short time gap between shocks.
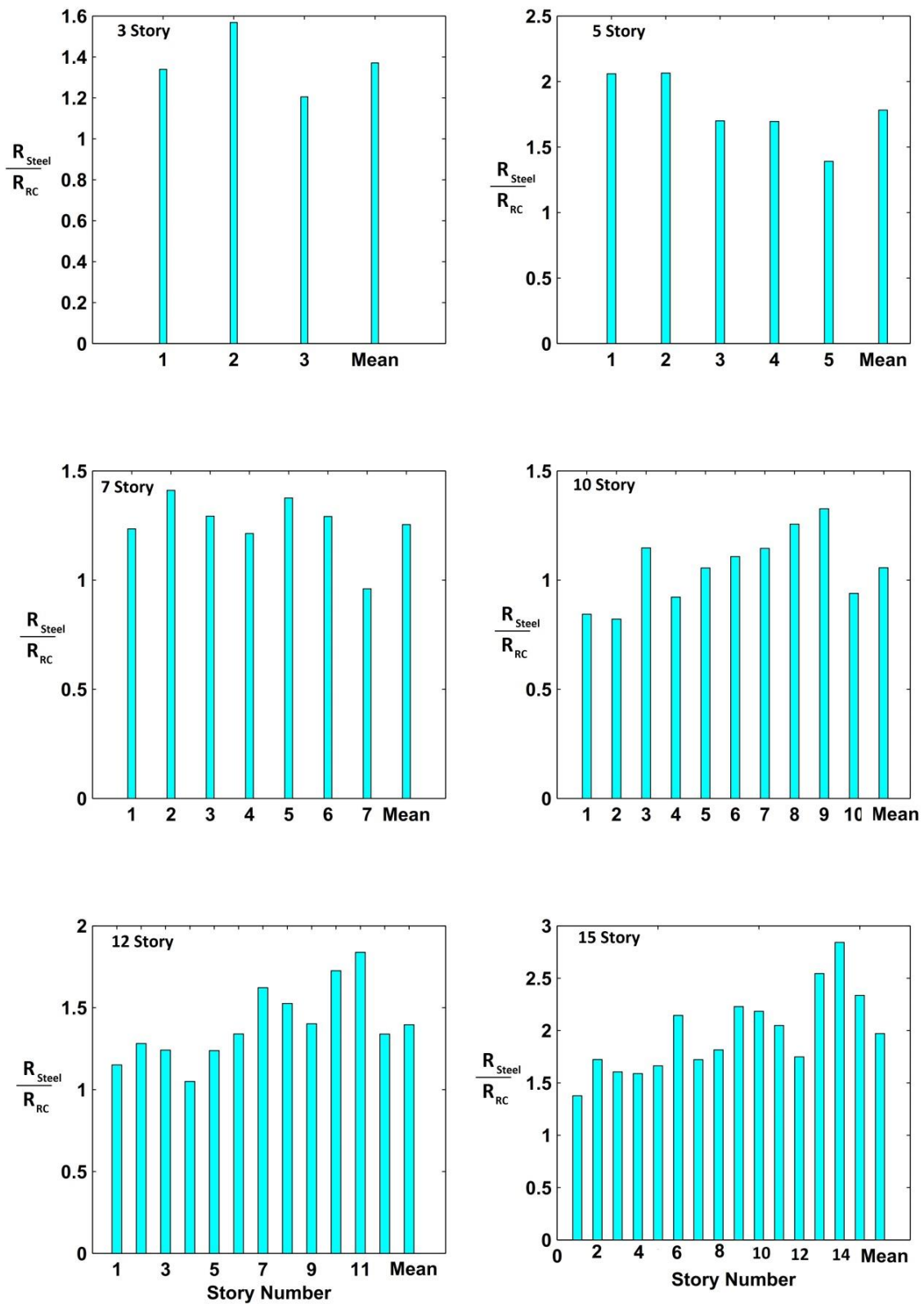
Fig. 10. Average of the DI ratio for steel to RC frames (R_{Steel}/R_{RC}) against all critical earthquakes.

- In the most severe conditions, increased damages of short and medium steel frames are about 57%, 94%, 42%, 33% and 84% more than those of RC frame under critical consecutive earthquakes. Moreover, additional damage in steel frames with 15 stories is about 1.84 times reinforced concrete frames.
- The average of the increased damage index ratio for steel to RC frames is always larger than one for all stories which presents the more suitable performance of RC frames rather than steel frames under consecutive earthquakes. Generally discarding the number of stories, results reveal that RC frames is 48% less vulnerable rather than the steel frames against the critical earthquakes with sequence phenomena.

REFERENCES

[1] Di Sarno, L., Ren Wu, J. (2021). "Fragility assessment of existing low-rise steel moment-resisting frames with masonry in fills under mainshock-aftershock earthquake sequences." Bulletin of Earthquake Engineering, 19: 2483–2504.

[2] Trevlopoulos, K., Gueguen, P., Helmstetter, A., Cotton, F. (2020). "Earthquake risk in reinforced concrete buildings during aftershock sequences based on period elongation and operational earthquake forecasting." Structural Safety, 2020, 84, 101922.

[3] Shi, F., Saygili, G., Ozbulut, O., and Zhou, Y. (2020). "Risk-based mainshock-aftershock performance assessment of SMA braced steel frames." Engineering Structures, Volume 212, 1 June 2020, 110506.

[4] Yang, F., Wang, G., and Ding, Y (2019). "Damage demands evaluation of reinforced concrete frame structure subjected to near-fault seismic sequences." Natural Hazards, 97:841–86.

[5] Jalayer, F., Ebrahimian, H. (2017). "Seismic risk assessment considering cumulative damage due to aftershocks." Earthquake Engineering & Structural Dynamics, 2017, 46(3), 369-389.

[6] Zhang, L., Goda, K., Luca, F. D., De Risi, R. (2020). "Mainshock-aftershock state-dependent fragility curves: A case of wood-frame houses in British Columbia, Canada." Earthquake Engineering Structural Dynamic, 2020, 1–20.

[7] Wen, W., Ji, D., Zhai, C. H. (2020). "Cumulative Damage of Structures under the Mainshock-aftershock Sequences in the Near-fault Region, Journal of Earthquake Engineering." Published online, 30 Apr 2020. DOI:0.1080/13632469.2020.1754307

[8] Zhai, C. H., Bao, X., Zheng, Z., Wang, X. (2018). "Impact of aftershocks on a post-mainshock damaged containment structure considering duration." Soil Dynamics and Earthquake Engineering, 2018, 115: 129–141.

[9] Wen, W., Ji, D., Zhai, C. H., Li, X., Sun, P. (2018). "Damage spectra of the mainshock-aftershock ground motions at soft soil sites." Soil Dynamics and Earthquake Engineering, 2018, 115: 815–825.

[10] Zhang, Y., Chen, J., Sun, C. H. (2017). "Damage-based strength reduction factor for nonlinear structures subjected to sequence-type ground motions." Soil Dynamics and Earthquake Engineering, 2017, 92: 298–311.

[11] Ghaderi, M., and Gholizadeh, S. (2021). "Mainshock–aftershock low-cycle fatigue damage evaluation of performance-based optimally designed steel moment frames." Engineering Structures, 237, 15 June 2021, 112207.

[12] Pan, H., and Kusunoki, K. (2020). "Aftershock damage prediction of reinforced-concrete buildings using capacity spectrum assessments." Soil Dynamics and Earthquake Engineering, 129 (2020) 105952.

[13] Ghodrati Amiri, G., Rajabi, E. (2018). "Effects of Consecutive Earthquakes on Increased Damage and Response of Reinforced Concrete Structures."

Computers and Concrete, 2018, 21(1): 55-66.

[14] Park, Y. J., Ang, A. H. (1985). "Mechanistic Seismic Damage Model for Reinforced Concrete." Journal of Structure, 1985, ASCE 111(4): 722-739.

[15] Ghodrati Amiri, G., Manouchehri Dana, F. (2005). "Introduction of the most suitable parameter for selection of critical earthquake." Computers & Structures, 2005, 83(8-9), 613-626.

[16] PEER, PEER NGA Database, Pacific Earthquake Engineering Research Center, University of California, Berkeley, California, 2017.

[17] USGS, United States Geological Survey's (USGS) Earthquake Hazards Program, 2015.

[18] Ghodrati Amiri, G., Rajabi, E. (2017). "Damage Evaluation of Reinforced Concrete and Steel Frames under Critical Successive Scenarios." International Journal of Steel Structures, 2017, 17(4): 1495-1514.

[19] Vamvatsikos, D., Cornell, C. A. (2002). Incremental dynamic analysis, Earthquake Engineering and Structural Dynamics, 2002, 31(3): 491–514.

[20] Hancock, J., Bommer, J. J., Stafford, P. J. (2008). "Numbers of scaled and matched accelerograms required for inelastic dynamic analyses." Earthquake Engineering and Structural Dynamic, 2008, 37, 1585-1607.

[21] Atkinson, G. M. (2009). "Earthquake Time Histories Compatible with the 2005 NBCC Uniform Hazard Spectrum." Canadian Journal of Civil Engineering, 36(6): 991-1000.

[22] Lignos, D. G., Hikino, T., Matsuoka, Y., Nakashima, M. (2013). "Collapse Assessment of Steel Moment Frames Based on E-Defense Full-Scale Shake Table Collapse Tests." Journal of Structural Engineering, 139(1): 120-132. DOI: 10.1061/(ASCE)ST. 1943-541X.0000608.

[23] Nagae, T., Ghannoum, W. M., Kwon, J., Tahara, K., Fukuyama, k., Matsumori, T., Shiohara, H., Kabeyasawa, T., Kono, S., Nishiyama, M., Saus, R., Wallace, J. W., Moehle, J. P. (2015). "Design Implications of Large-Scale Shake-Table Test on Four-Story Reinforced Concrete Building." ACI STRUCTURAL JOURNAL, TECHNICAL PAPER. ACI Structural Journal, 112(1-6): 135-146, MS No. S-2013-022.R2, Doi: 10.14359/51687421. American Concrete Institute.

[24] Haselton, C., Taylor Lange, A., Liel, B., Deierlein, G. G. (2007). "Beam-Column Element Model Calibrated for Predicting Flexural Response Leading to Global Collapse of RC Frame Buildings." Report No. PEER Report 2007/03. Berkeley Pacific Earthquake Engineering Research Center College of Engineering, University of California.

[25] Moehle, J. K., Mahin, S., Bozorgnia, Y. (2010). "Modeling and Acceptance Criteria for Seismic Design and Analysis of Tall Buildings." PEER/ATC-72-1. Repared by APPLIED TECHNOLOGY COUNCIL Courtesy of Joseph Maffei, Rutherford & Chekene, San Francisco, California, 2010.

[26] Ibarra, L. F., Media, R. A., Krawinkler, H. (2005). "Hysteretic models that incorporate strength and stiffness deterioration." Earthquake Engineering and Structural dynamics, 2005, 34:1489–1511.

[27] Fan, Y., Guo, Z., Zhao, P., and Yu, B. (2021). "Experimental Study of Seismic Damage with Park-Ang Model for Recycled Aggregate Concrete Columns." KSCE J Civ Eng (2021). https://doi.org/10.1007/s12205-021-1110-x.

[28] Hait, P., Sil, A., and Choudhury, S. (2021). "Prediction of global damage index of reinforced concrete building using artificial neural network." International Journal for Computational Methods in Engineering Science and Mechanics. Doi: 10.1080/15502287.2021.1887405.

[29] Lakhade, S. O., Kumar, R., Jaiswal, O. R. (2020). "Estimation of drift limits for different seismic damage states of RC

frame staging in elevated water tanks using Park and Ang damage index." Earthquake Engineering and Engineering Vibration, 2020, 19:161–177.

[30] Payganeh, M. B., Mortezaei, A. (2020). "Seismic Damage Assessment of RC Buildings Subjected to the Rotational Ground Motion Records Considering Soil-Structure Interaction." Journal of Rehabilitation in Civil Engineering 8-2 (2020) 62-80.

[31] Carrillo, J., Vera, S. O., Blandonc, C. (2019). "Damage assessment of squat, thin and lightly-reinforced concrete walls by the Park & Ang damage index." Journal of Building Engineering 26 (2019) 100921. Doi: 100921. 10.1016/j.jobe.2019.100921.

[32] Hatzivassiliou, M., Hatzigeorgiou, G. D. (2015). "Seismic sequence effects on three-dimensional reinforced concrete buildings." Soil Dynamics and Earthquake Engineering, 2015, 72: 77 – 88.

[33] Park, Y. J., Reinhorn, A. M., Kunnath, S. K. (1987). IDARC: Inelastic Damage Analysis of Frame Shear-Wall Structures, Technical Report NCEER-87-0008, National Center for Earthquake Engineering Research, State University of NewYork at Buffalo, NY, 1987.

[34] Ghosh, S., Datta, D., Katakdhond, A. A. (2011). "Evaluation of the Park-Ang damage index for planar multi-story frames using equivalent single-degree system". Engineering Structures, 2011, 33: 2509-2524.

[35] Sorace, S. (1998). "Seismic damage assessment of steel frames." Journal of Structural Engineering, 1998, 124(5).

P. Appendix:

P.1 Structural modeling

As mentioned in Section (2.2), steel and concrete intermediate moment resisting frames consisting of 3, 5, 7, 10, 12, 15 stories and fixed base columns are designed with considering the stiffness and strength deterioration and analyzed under significant number of as-recorded critical seismic scenarios with/without sequences in OpenSees software. These frames are verified by the analytical and experimental results of parametric study by Lignos et al. [22] for steel frames and Nagae et al. [23] for RC frames which have been tested on the E-Defense shake table provided by E-Defense company –National Research Institute for Earth Science and Disaster Prevention (NIED)– in Japan. The geometric and material properties of the designed frames are presented in Tables P.1, 2 and 3. Beams with concentrated plastic hinges and columns with fiber section are employed to simulate the nonlinear flexural behavior of the moment frames. In this regard, modeling of the beams is performed using "beam with hinges element", an elastic material was assigned to the mid span and a specific length (height of beam) at both ends is allocated to the plastic hinges. Backbone curve for suggested by Ibarra [24] for concrete beam elements and Ibarra-Krawinkler [25] for steel beam elements, is shown in Fig. P1.

The tri-linear Ibarra model, as mentioned in Section (2-2), was employed in the Open Sees platform using the Clough material proposed by Altoontash [24]. Then uniaxial sections with pre-defined M-θ according to the Clough material were assigned to the plastic hinges.

Columns are modeled by means of the "fiber method" with the capability of developing distributed plasticity along the length of the element because flexural behavior in the columns is highly dependent on the interaction of their axial and bending forces. However, the aforementioned approach is not able to consider variable axial forces for beams during the analysis.

As a result, the fiber sections are assigned to the "nonlinear Beam Column elements". Each element was also divided into four sub-elements in a story level to provide more robustness. Also, uniaxial material

concrete02 and steel02 are used for reinforced concrete. In steel frames, uniaxial material hardening is used for implementation of column elements.

Table P1. Geometric properties of the designed RC frames.

Number of story	Level	Column Width (cm)	Column Height (cm)	Beam Width (cm)	Beam Height (cm)
3	1, 2, 3	40	40	40	35
5	1, 2	50	50	50	40
	3, 4, 5	40	40	50	40
7	1, 2, 3, 4	55	55	55	45
	5, 6, 7	45	45	45	35
10	1, 2, 3, 4	55	55	55	40
	5, 6, 7	45	45	45	40
	8, 9, 10	40	40	40	35
12	1, 2, 3, 4	60	60	60	50
	5, 6, 7, 8	55	55	55	40
	9, 10, 11, 12	40	40	40	35
15	1, 2, 3, 4	65	65	65	50
	5, 6, 7, 8	55	55	55	50
	9, 10, 11, 12	45	45	45	40
	13, 14, 15	35	35	35	35

Table P2. Geometric properties of the designed steel frames.

Number of story	Level	Column section	Beam section
3	1, 2, 3	W27×146	W24×131
5	1, 2	W27×129	W24×117
	3, 4, 5	W24×192	W21×101
7	1, 2, 3, 4	W27×146	W24×117
	5, 6, 7	W24×192	W21×39
10	1, 2, 3, 4	W30×173	W27×129
	5, 6, 7	W27×146	W24×117
	8, 9, 10	W24×146	W21×48
12	1, 2, 3, 4	W33×354	W30×148
	5, 6, 7, 8	W33×318	W30×108
	9, 10, 11, 12	W24×370	W24×146
15	1, 2, 3, 4	W36×300	W33×152
	5, 6, 7, 8	W33×354	W30×148
	9, 10, 11, 12	W33×318	W30×108
	13, 14, 15	W24×370	W24×146

Table P3. Material properties of the designed 3, 5, 7, 10, 12 and 15 story frames.

Concrete	Specified Concrete Compression Strength f_c (kg/cm^2)	Modulus of Elasticity, E (kg/cm^2)	Yield Stress, F_y (kg/cm^2)
	250	2.388 e+5	4000
Steel	Modulus of Elasticity, E (kg/cm^2)	Tensile Stress, F_u (kg/cm^2)	Yield Stress, F_y (kg/cm^2)
	2.039 e+6	3700	2400
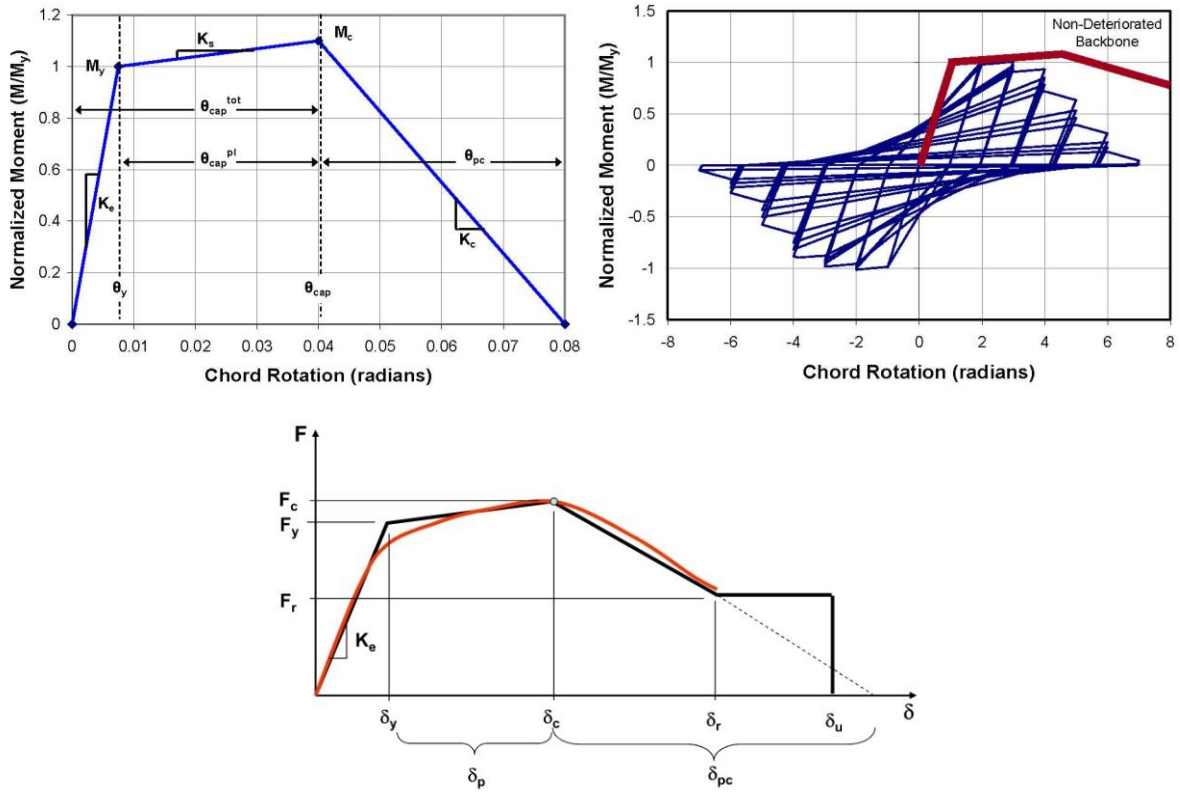
Fig. P1. The schematic of Tri-linear backbone curve suggested by Ibarra [24]-up, backbone curve of the Ibarra-Krawinkler model [25]- bottom.